Minerals **2017**, *7*, 140; doi:10.3390/min7080140

Supplementary Material

Physicochemical and Additive Controls on the Multistep Precipitation Pathway of Gypsum

Mercedes Ossorio, Tomasz M. Stawski, Juan Diego Rodriguez-Blanco, Mike Sleutel, Juan Manuel Garcia-Ruiz, Liane G. Benning and Alexander E. S. Van Driessche

S1. Gypsum Standard

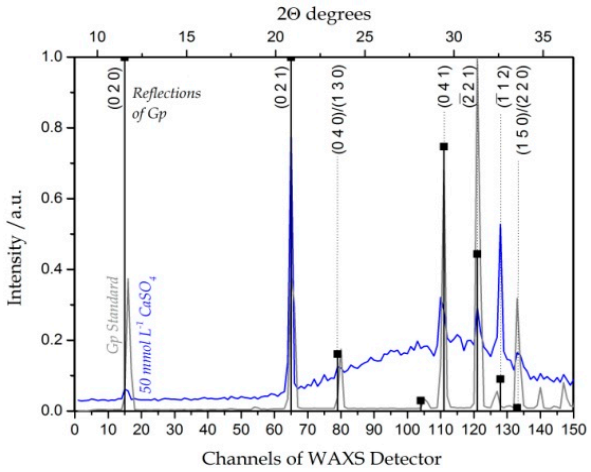

Figure S1. Diffraction patterns of commercial gypsum (gray) used as standard, together with a diffraction pattern (blue) of the solid phase formed from a 50 mmol·L^{-1} $CaSO_4$ solution at 21 °C after 3.3 h of reaction. The analyzed reflections of gypsum (black; pattern PDF2: 33–311) are indicated.

S2. Estimation of the Crystallite Size of Gypsum

The crystallite size was estimated for the (020), (021), (041) and (21) reflections of gypsum (space group C2/c). The diffraction peaks corresponding to all these reflections were fitted using the pseudo Voigt function, and full width at half maximum (FWHM) values were estimated for each of these diffraction peaks of the gypsum patterns. On the other hand, the intrinsic angle-dependent instrumental broadening of the 2D WAXS detector was obtained by measuring the FWHM of the diffraction peaks of a highly crystalline Si standard (NIST 640c) and interpolating the missing values for all the diffraction angles within the range using a spline function. The interpolated, and if available actual, angle-dependent FWHMs from the Si diffraction patterns were subtracted from the measured FWHM for the obtained gypsum diffraction patterns. Finally, the resulting FWHM values (only corresponding to the sample contribution to the peak broadening) were used to derive the crystallite size of gypsum using the Scherrer equation. Crystallite sizes of gypsum were estimated until the moment at which reactions were considered complete (i.e., when no further changes in the intensity of the diffraction peaks was observed).

The Scherrer equation is only applicability for small crystallite sizes. This is a direct consequence of the difficulty of measuring very precisely the FWHM. The estimated error for the FWHM determination is 0.05°, although the resolution of diffraction pattern is determined by the detector, which is approximately 0.25° (150 Channels for ~40°). Figure S2 illustrates the relation through the Scherrer equation between the peak broadening (with peak broadening $B = FWHM_{sample} - FWHM_{Si}$) and the crystallite size, given by:

$$B = \frac{K \cdot \lambda}{L \cdot \cos\theta} \quad \text{(S1)}$$

where K is a shape factor (1 for spherical particles), the wavelength λ in synchrotron radiation is 0.1 nm, L is the crystallite size (nm), and θ is the X-ray angle (°). By dividing the average error of the FWHM measurements (0.05°) with the slope between peak broadening and crystallite size (Figure S2), the error in crystallite size can be estimated. A small error in the FWHM results in a large error in the estimated crystallite size and this effect increases with increasing crystallite size, as shown in Table S1. Therefore, crystallite size estimations by employing the Scherrer equation is only meaningful for small crystallite sizes (<~20 nm).

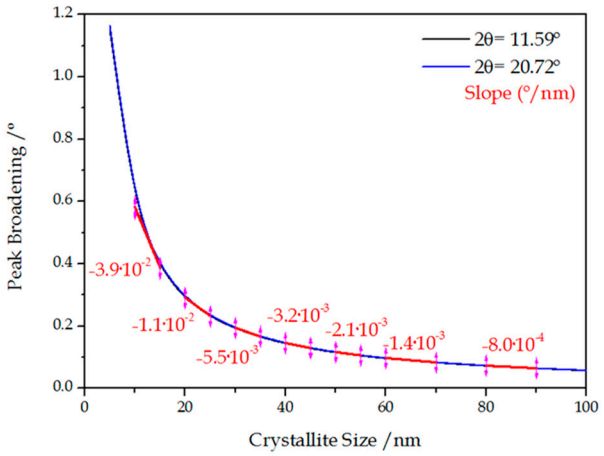

Figure S2. Relation between peak broadening and crystallite size for two of the main reflections of gypsum; (020) at 2θ = 11.59°, and (021) at 2θ = 20.72°. The variations in the slope (°/nm) of these curves with increasing crystallite size are also indicated (in red).

The averaged estimated crystallite size from the different gypsum reflections (020), (021), (041) and (021) showed a similar size, i.e. >100 nm (Table S2). The same order of size was found for all the analyzed datasets and remained almost invariable from the beginning (i.e., when the WAXS signal starts appearing) to the end of the experiments. Hence, the applicability of the Scherrer equation in this case is meaningless due to the disproportionate errors associated to these large crystallite sizes and low resolution of the WAXS detector.

Table S1 Estimation of the approximate errors associated to crystallite sizes from 10 to 85 nm.

Crystallite Size /nm	Calculated Error /nm
10	1.28
20	4.55
30	9.09
40	15.63
50	23.81
65	35.71
85	62.50

Table S2 Estimation of the crystallite size for the (020) reflection of gypsum.

[$CaSO_4$] /mmol·L^{-1}	*T* /°C	Additives	Averaged Crystallite Size * /nm
50	4	N.A.	155
50	12	N.A.	184
50	21	N.A.	165
50	30	N.A.	197
50	40	N.A.	187
75	21	N.A.	212
75	21	citrate	179
75	21	Mg	235
100	21	N.A.	198
100	21	citrate	318
100	21	Mg	223
150	21	N.A.	138
150	21	citrate	318
150	21	Mg	217

* Errors associated to the crystallite size are not indicated since these large crystallite size values present very large errors. N.A. = Not Applicable

S3. Reaction Rates and Induction Times of Gypsum Formation

The rate constants, *k,* were obtained from fitting the WAXS data using Eqation (1).

Table S3. 50 mmol·L^{-1} $CaSO_4 \cdot 2H_2O$. Precipitation from pure aqueous solution.

50 mmol·L^{-1} $CaSO_4$, Pure Aqueous Solution (*n* = 1)						
Reflection of Gp (020)	*T*/°C	4	12	21	30	40
	t_{ind}/s	2400	1800	1250	700	700
	k/s^{-1} (10^{-4})	1.58	1.94	2.55	4.85	8.98
	R^2	0.95059	0.92925	0.97695	0.95944	0.72293
Reflection of Gp (041)	*T*/°C	4	12	21	30	40
	t_{ind}/s	1400	1700	1000	700	225
	k/s^{-1} (10^{-4})	1.83	1.88	3.04	5.12	8.75
	R^2	0.88499	0.94765	0.93393	0.95728	0.98520
Reflection of Gp (021)	*T*/°C	4	12	21	30	40
	t_{ind}/s	-	1570	900	600	180
	k/s^{-1} (10^{-4})	-	3.39	3.93	6.42	9.36
	R^2	-	0.99905	0.89343	0.94740	0.97086

Table S4. 75 mmol·L^{-1} $CaSO_4 \cdot 2H_2O$, at 21 °C. Precipitation in pure aqueous solution and in presence of additives in solution

75 mmol·L^{-1} $CaSO_4$, 21 °C (n = 1)				
	Experimental Condition	Pure system	Mg^{2+} ions	citric acid
Reflection of Gp (020)	t_{ind}/s	125	600	450
	k/s^{-1} (10^{-4})	36.00	7.91	13.00
	R^2	0.80743	0.92037	0.74621
	Experimental Condition	Pure system	Mg^{2+} ions	citric acid
Reflection of Gp (041)	t_{ind}/s	140	500	400
	k/s^{-1} (10^{-4})	35.00	8.04	14.60
	R^2	0.70713	0.91940	0.80551
	Experimental Condition	Pure system	Mg^{2+} ions	citric acid
Reflection of Gp (021)	t_{ind}/s	120	600	450
	k/s^{-1} (10^{-4})	34.00	9.34	13.50
	R^2	0.81352	0.89623	0.73358

Table S5. 100 mmol·L^{-1} $CaSO_4 \cdot 2H_2O$, at 21 °C. Precipitation in pure aqueous solution and in presence of additives in solution.

100 mmol·L^{-1} $CaSO_4$, 21 °C (n = 1)				
	Experimental Condition	Pure system	Mg^{2+} ions	citric acid
Reflection of Gp (020)	t_{ind}/s	60	380	150
	k/s^{-1}(10^{-4})	61.80	15.00	32.10
	R^2	0.95846	0.93964	0.83343
	Experimental Condition	Pure system	Mg^{2+} ions	citric acid
Reflection of Gp (041)	t_{ind}/s	50	250	150
	k/s^{-1} (10^{-4})	65.80	14.50	30.40
	R^2	0.97614	0.93348	0.92814
	Experimental Condition	Pure system	Mg^{2+} ions	citric acid
Reflection of Gp (021)	t_{ind}/s	60	250	150
	k/s^{-1} (10^{-4})	64.30	18.20	33.90
	R^2	0.95380	0.91128	0.90968

Table S6. 150 mmol·L^{-1} $CaSO_4 \cdot 2H_2O$, at 21 °C. Precipitation from a pure solution and in the presence of additives.

150 mmol·L^{-1} $CaSO_4$, 21 °C (n = 1)				
Reflection of Gp (020)	Experimental Condition	Pure system	Mg^{2+} ions	citric acid
	t_{ind}/s	40	150	60
	k/s^{-1} (10^{-4})	115.90	25.80	80.10
	R^2	0.94706	0.82773	0.98964
Reflection of Gp (041)	Experimental Condition	Pure system	Mg^{2+} ions	citric acid
	t_{ind}/s	40	120	60
	k/s^{-1} (10^{-4})	115.10	31.90	101.20
	R^2	0.88949	0.88010	0.97627
Reflection of Gp (021)	Experimental Condition	Pure system	Mg^{2+} ions	citric acid
	t_{ind}/s	40	120	60
	k/s^{-1} (10^{-4})	115.90	39.20	109.80
	R^2	0.92103	0.92601	0.97374

S4. Calculation of the Activation Energy for Gypsum in a 50 mmol·L^{-1} $CaSO_4$ Solution

The activation energy for gypsum was derived from our experimental data by employing the Arrhenius´s equation, $\ln k = \ln A - (E_A/RT)$; where k is the rate constant, A is the pre-exponential factor, E_A is the activation energy, R is the global gas constant (8.314 J·K^{-1}·mol^{-1}), and T is the absolute temperature. When plotting $\ln k$ versus ($1/T$) (Figure 3), the activation energy E_A can be calculated from the linear fitting of the data;

(a) (020) reflection of gypsum; b = −4230.54; E_A = 35.17 kJ·mol^{-1}

(b) (041) reflection of gypsum; b = −3983.66; E_A = 33.12 kJ·mol^{-1}

(c) (021) reflection of gypsum; b = −2990.39; E_A = 24.86 kJ·mol^{-1}

S5. Evolution of Mg^{2+} and Ca^{2+} Concentration in Solution During Gypsum Precipitation

A 50 mmol·L^{-1} $CaSO_4$ solution at 21 °C was sampled at different times of reaction for ion chromatography (IC) analyses in order to determine the absolute concentration of ions ($Ca^{2+}$and Mg^{2+}) in solution at each stage of the reaction (Figure S3).

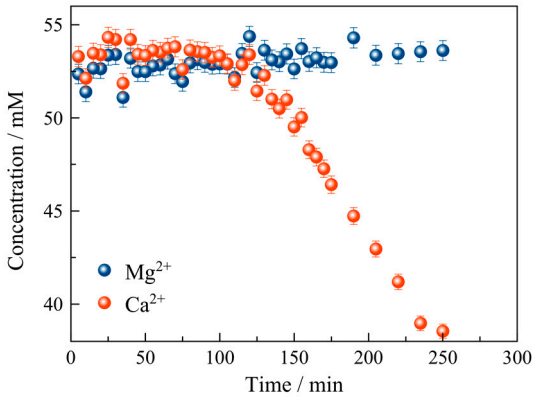

Figure S3. Variation in the concentration of Ca^{2+} and Mg^{2+} ions analyzed by IC (dots), during the off-line precipitation from a 50 mmol·L^{-1} $CaSO_4$ solution at 21 °C.